Looking for signatures of Dirac dispersion in optical spectra

Alexander Yaresko

Max Planck Institute for Solid State Research,
Stuttgart, Germany

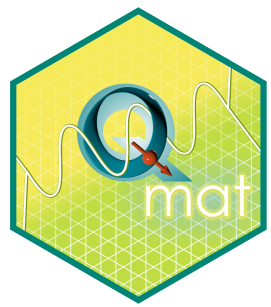

Ukratop, Dresden,
December 4–5, 2018

1. model optical conductivity
2. a quest for Weyl points in the $YbMnBi_2$
3. low energy peaks in optical conductivity of NbP
4. triple points in GdPtBi

accidental degeneracy of bands

AUGUST 15, 1937 PHYSICAL REVIEW VOLUME 52

Accidental Degeneracy in the Energy Bands of Crystals

CONYERS HERRING
Princeton University, Princeton, New Jersey
(Received June 16, 1937)

The circumstances are investigated under which two wave functions occurring in the Hartree or Fock solution for a crystal can have the same reduced wave vector and the same energy. It is found that coincidence of the energies of wave functions with the same symmetry properties, as well as those with different symmetries, is often to be expected. Some qualitative features are derived of the way in which energy varies with wave vector near wave vectors for which degeneracy occurs. All these results, like those of the preceding paper, should be applicable also to the frequency spectrum of the normal modes of vibration of a crystal.

- Symmetry inequivalent manifolds (bands) may cross.
- For crystals with an inversion center, contacts of equivalent manifolds $M^i(\mathbf{k})$, $M^j(\mathbf{k})$ may occur at all points $\mathbf{k}$ of an endless curve in $\mathbf{k}$-space
- For a crystal without an inversion center, contacts of equivalent manifolds $M^i(\mathbf{k})$, $M^j(\mathbf{k})$ may occur for isolated points $\mathbf{k}$, and such contacts cannot be destroyed by an infinitesimal change in the potential function V
- All kinds of contacts of equivalent manifolds except the ones described above are vanishingly improbable

1. model optical conductivity
2. a quest for Weyl points in the $YbMnBi_2$
3. low energy peaks in optical conductivity of NbP
4. triple points in GdPtBi

optical conductivity of 2D graphene

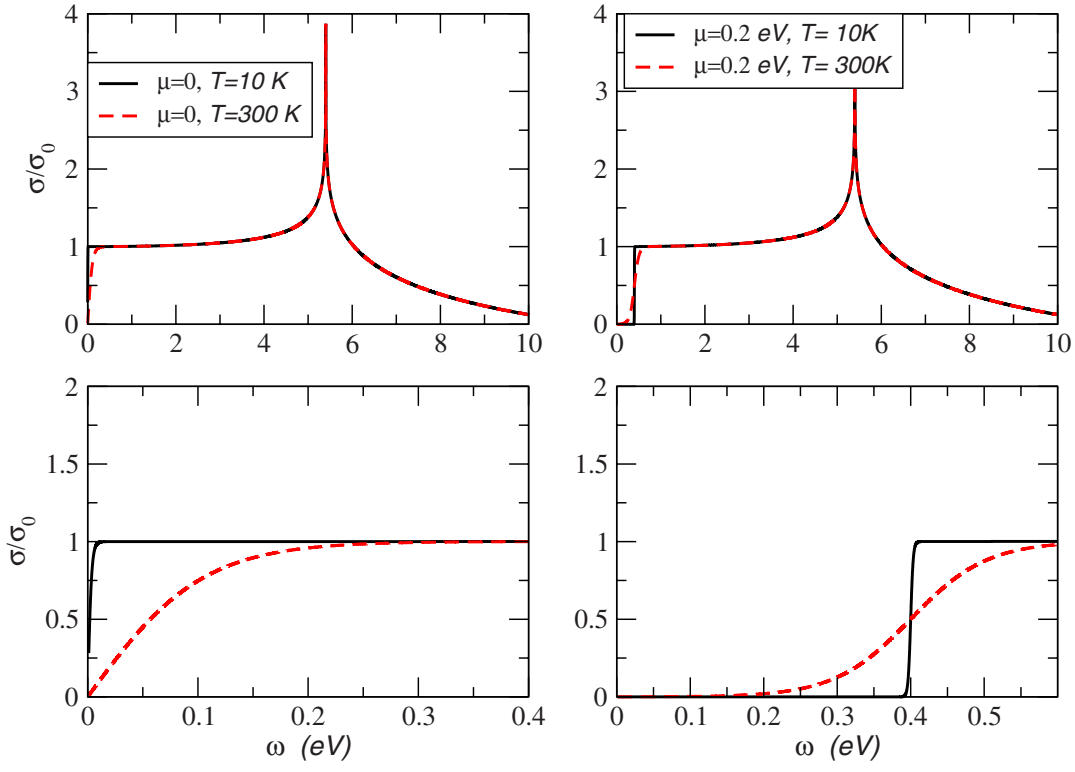

T. Stauber, *et al*, PRB **78**, 085432 (2008)

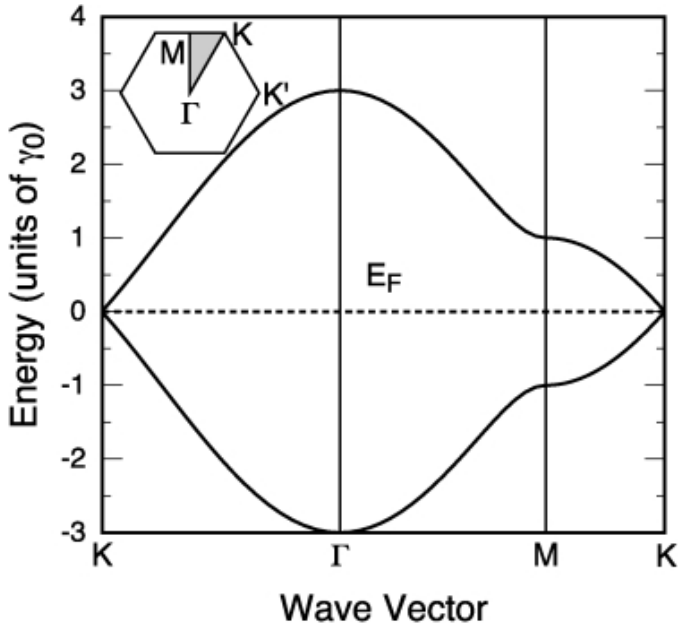

T. Ando, *et al*, jpsj **71**, 1318 (2002)

- constant $\sigma(\omega \to 0) = \sigma_0$ for $\mu = 0$
- step of $\sigma(\omega)$ at $\omega = 2\mu$ for $\mu \neq 0$
- $\sigma_0 = \frac{\pi}{2}\frac{e^2}{h}$ does not depend on t

3D Weyl semimetal

4×4 Hamiltonian: $H = v\tau_x \boldsymbol{\sigma}\cdot\mathbf{k} + m\tau_z + b\sigma_z = \begin{pmatrix} m\mathbb{I}+b\sigma_z & v\boldsymbol{\sigma}\cdot\mathbf{k} \\ v\boldsymbol{\sigma}\cdot\mathbf{k} & -m\mathbb{I}+b\sigma_z \end{pmatrix}$

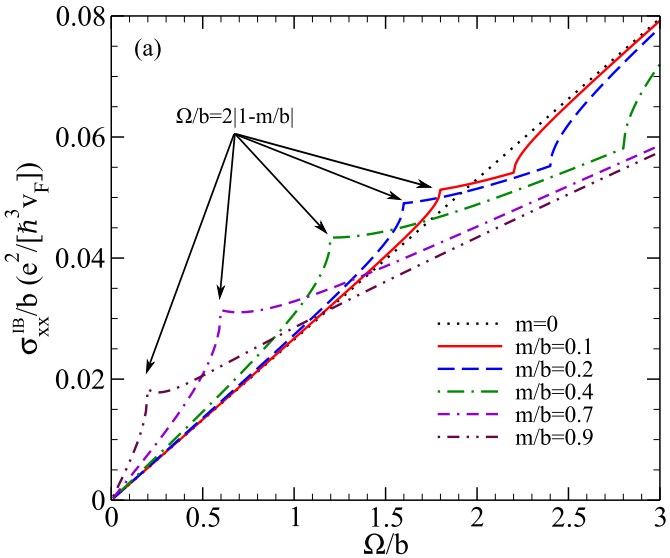

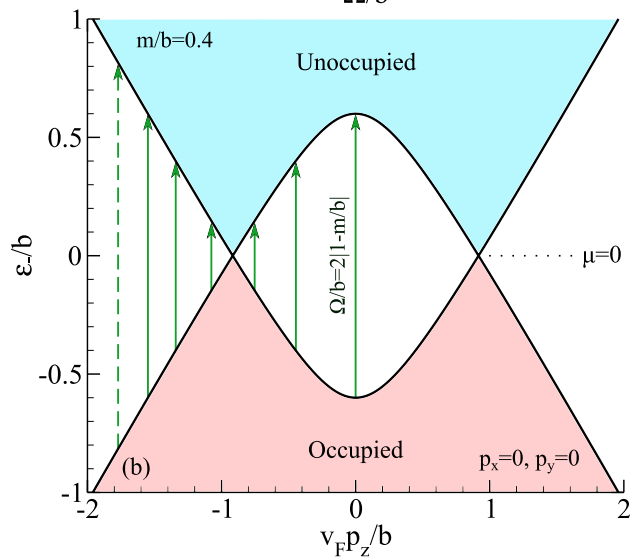

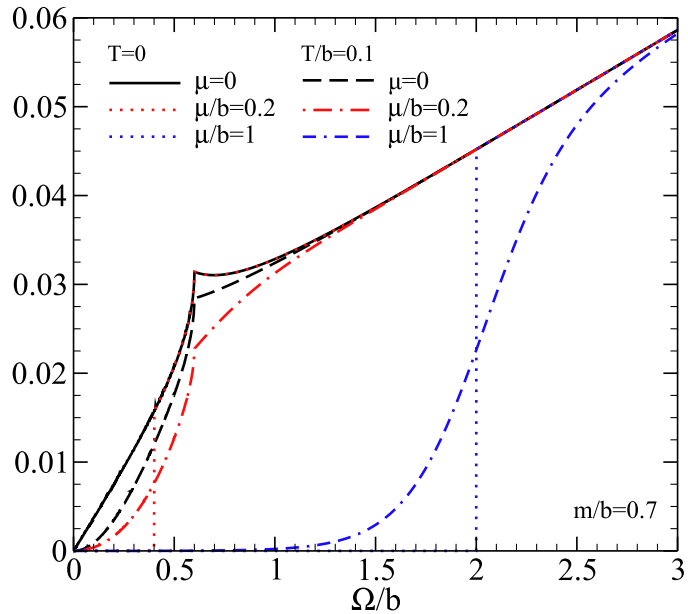

- linear $\sigma(\omega) \sim \omega$ at low photon energy
- a van Hove singularity at $\Omega/b = 2|1 - m/b|$
- Weyl semimetal when $b > m > 0$
- a Dirac cone at $b = m = 0$

C.J. Tabert and J.P. Carbotte, PRB **93**, 085442 (2016)

line node semimetal

4×4 Hamiltonian: $H = v\tau_x \boldsymbol{\sigma}\cdot\mathbf{k} + b\tau_z\sigma_x = \begin{pmatrix} b\sigma_x & v\boldsymbol{\sigma}\cdot\mathbf{k} \\ v\boldsymbol{\sigma}\cdot\mathbf{k} & -b\sigma_x \end{pmatrix}$

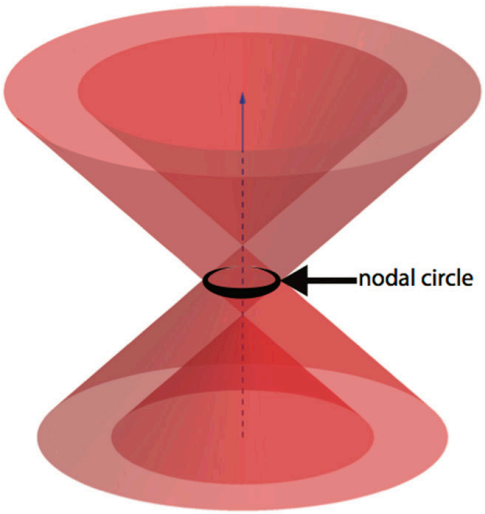

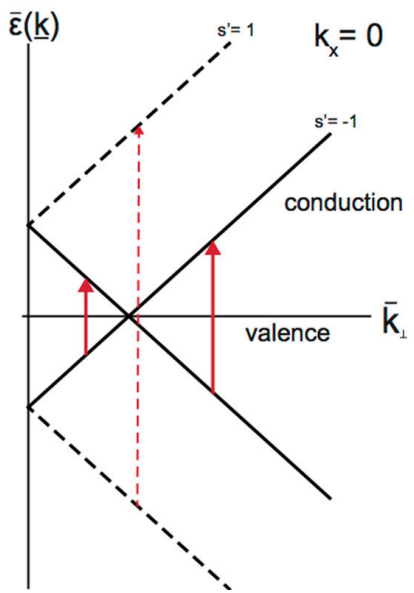

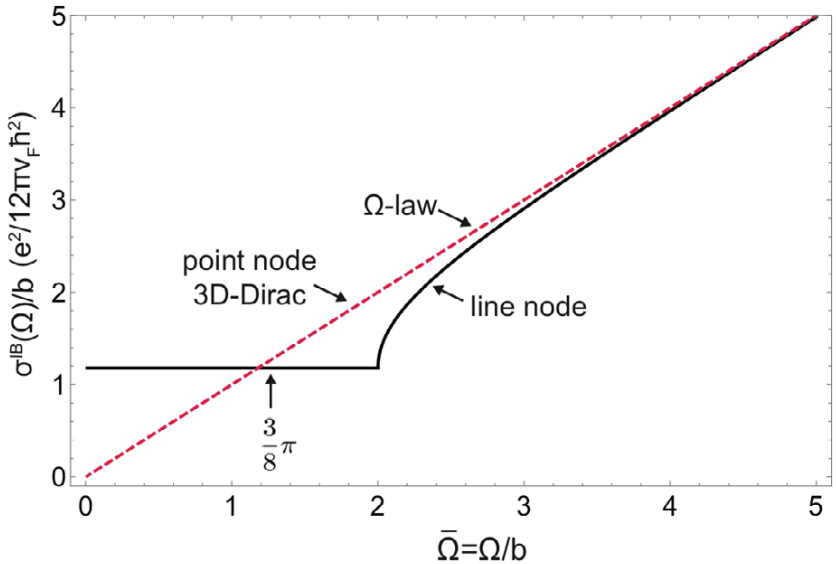

Figure 2. The interband optical conductivity as a function of photon energy $\bar{\Omega}$. Both quantities are scaled by b which makes the curve (solid black line) universal. The dashed red line is for comparison and applies to the point node 3D-Dirac case. Above $\bar{\Omega} \cong 3$, the two line and point node results merge. Below $\bar{\Omega} = 2$, the line node gives a constant response of height $3\pi/8$ in our units.

- $\sigma(\Omega) = \frac{3}{8}\pi b$ for $\Omega < 2b$
- $\sigma(\Omega) \sim \Omega$ for $\Omega \gtrsim 3b$

M. Koshino and I. Hizbullah, PRB **93**, 045201 (2016), J.P. Carbotte, JPCM **29**, 045301 (2017)

1. model optical conductivity
2. a quest for Weyl points in the $YbMnBi_2$
3. low energy peaks in optical conductivity of NbP
4. triple points in GdPtBi

crystal structure of $AMnBi_2$

YbMnBi$_2$, CaMnBi$_2$ ($P4/nmm$)

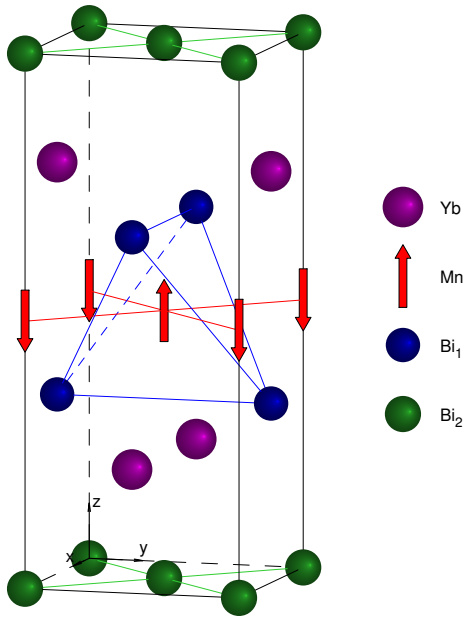

- Mn^{2+} ($3d^5$, $S_{5/2}$) in Bi_1 tetrahedra
- Mn: AFM order at ∼300K
- Ca^{2+}, Sr^{2+},Yb^{2+}($4f^{14}$), Eu^{2+}($4f^7$,$S_{7/2}$)
- square lattice of Bi_2

EuMnBi$_2$, SrMnBi$_2$($I4/mmm$)

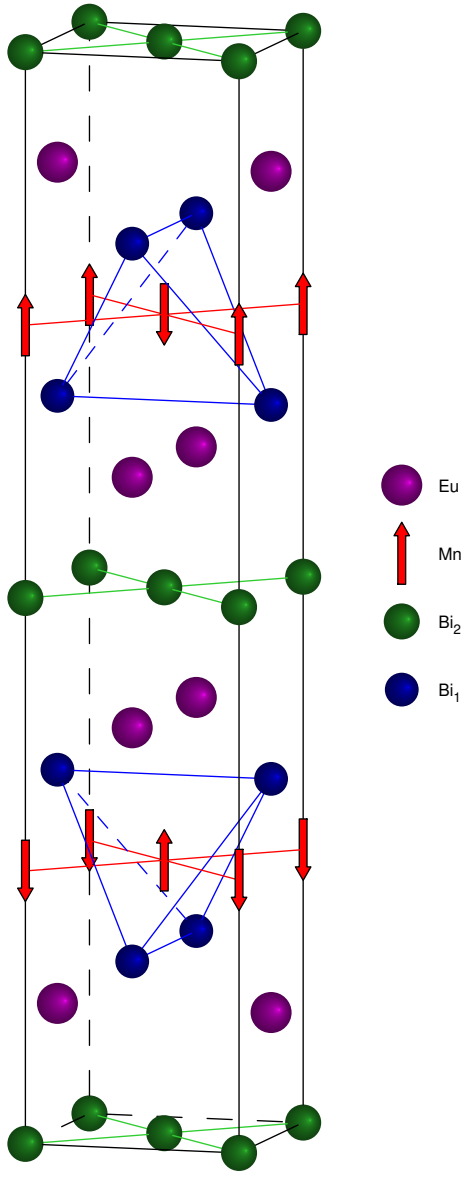

$YbMnBi_2$: Dirac bands without SOC and spin polarization

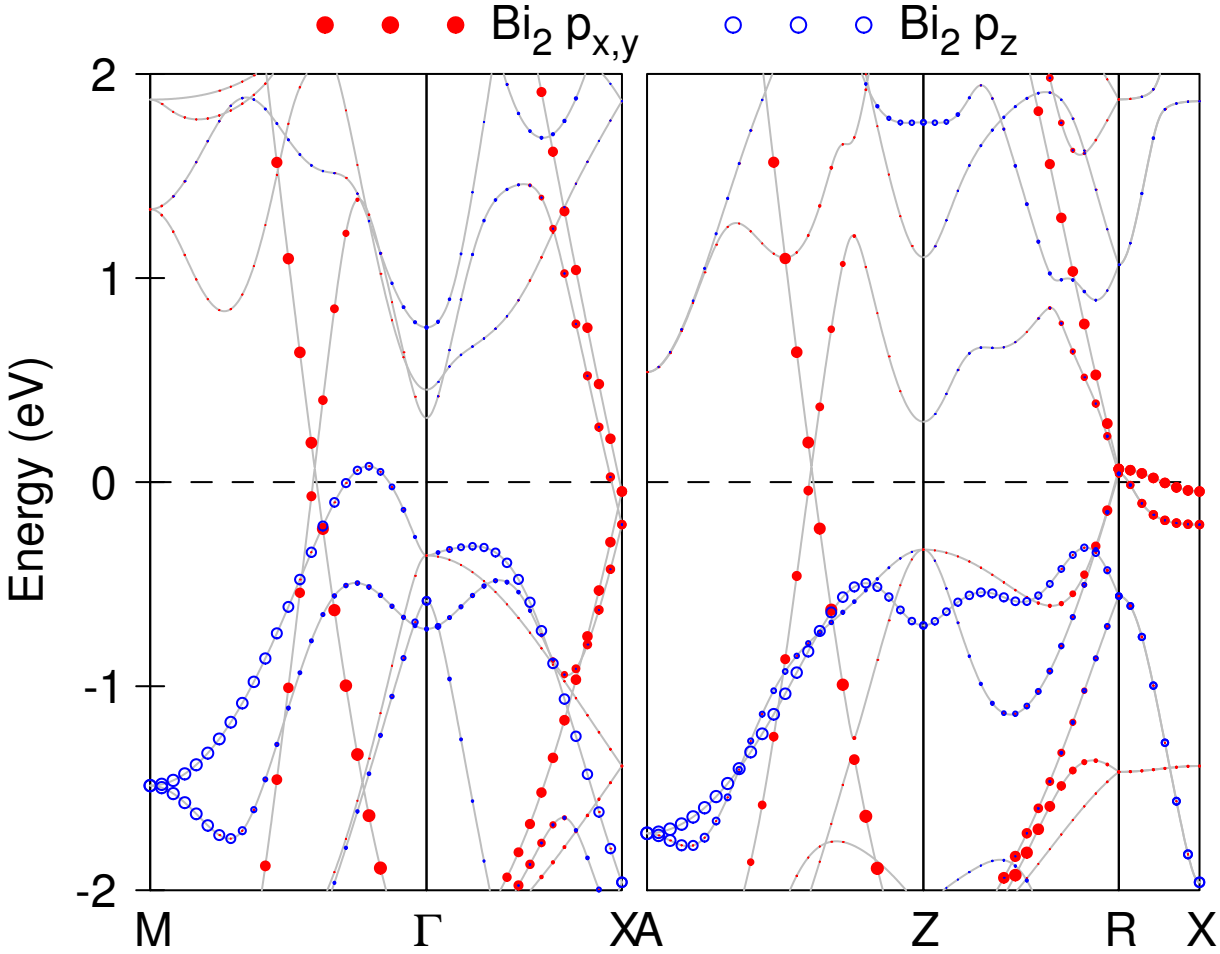

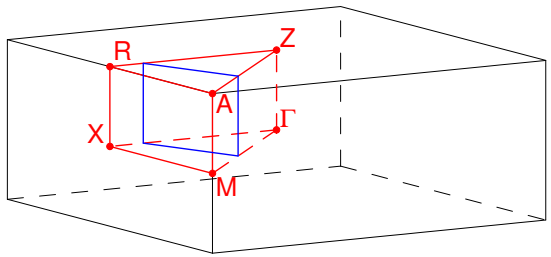

semi-core Yb $4f$, Mn $3d$

- Bi_2 p band crossing due to doubling of a 2D unit cell
- symmetry protected Dirac line nodes
- high velocity for Bi_2 $p_{x,y}$ bands ($\sim v$ in graphene) $\perp$ to Dirac lines
- much smaller velocity along a line

$YbMnBi_2$: SOC bands at E_F

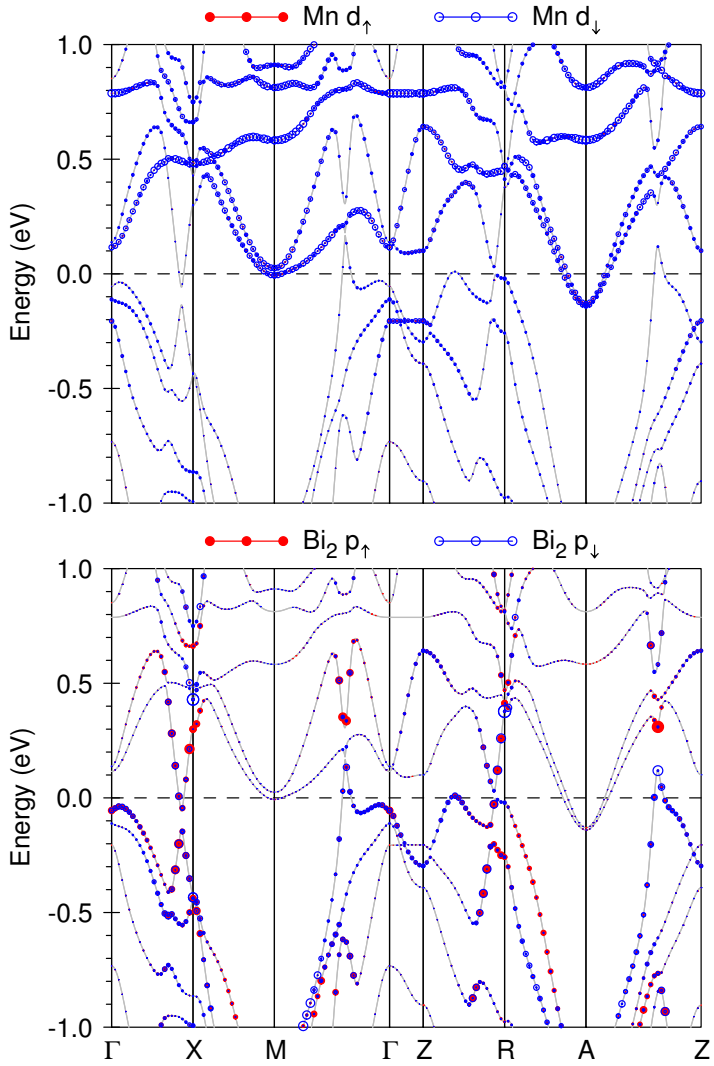

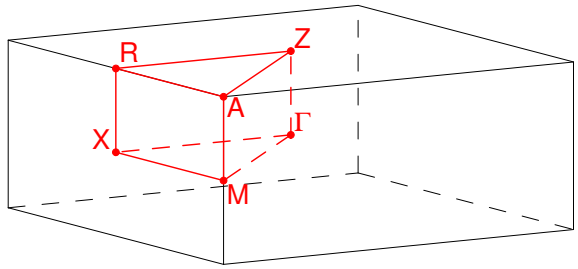

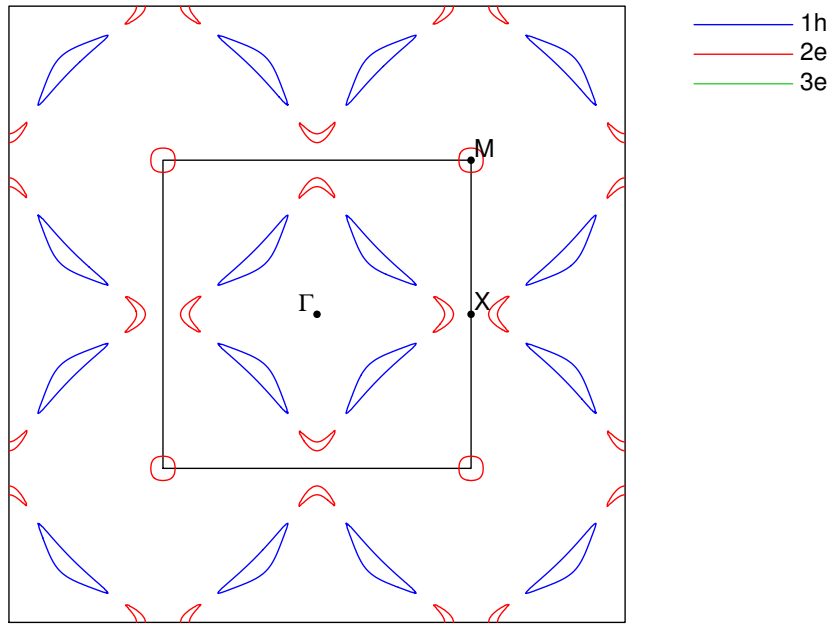

- T symmetry is broken but all bands are doubly degenerate because of TP
- Bi_2 p Dirac cones are gapped; h lenses (Γ–M), e boomerangs (Γ–X)
- Mn $d_\downarrow$ bands cross E_F near Γ–Z line

ARPES Fermi surface maps for $YbMnBi_2$

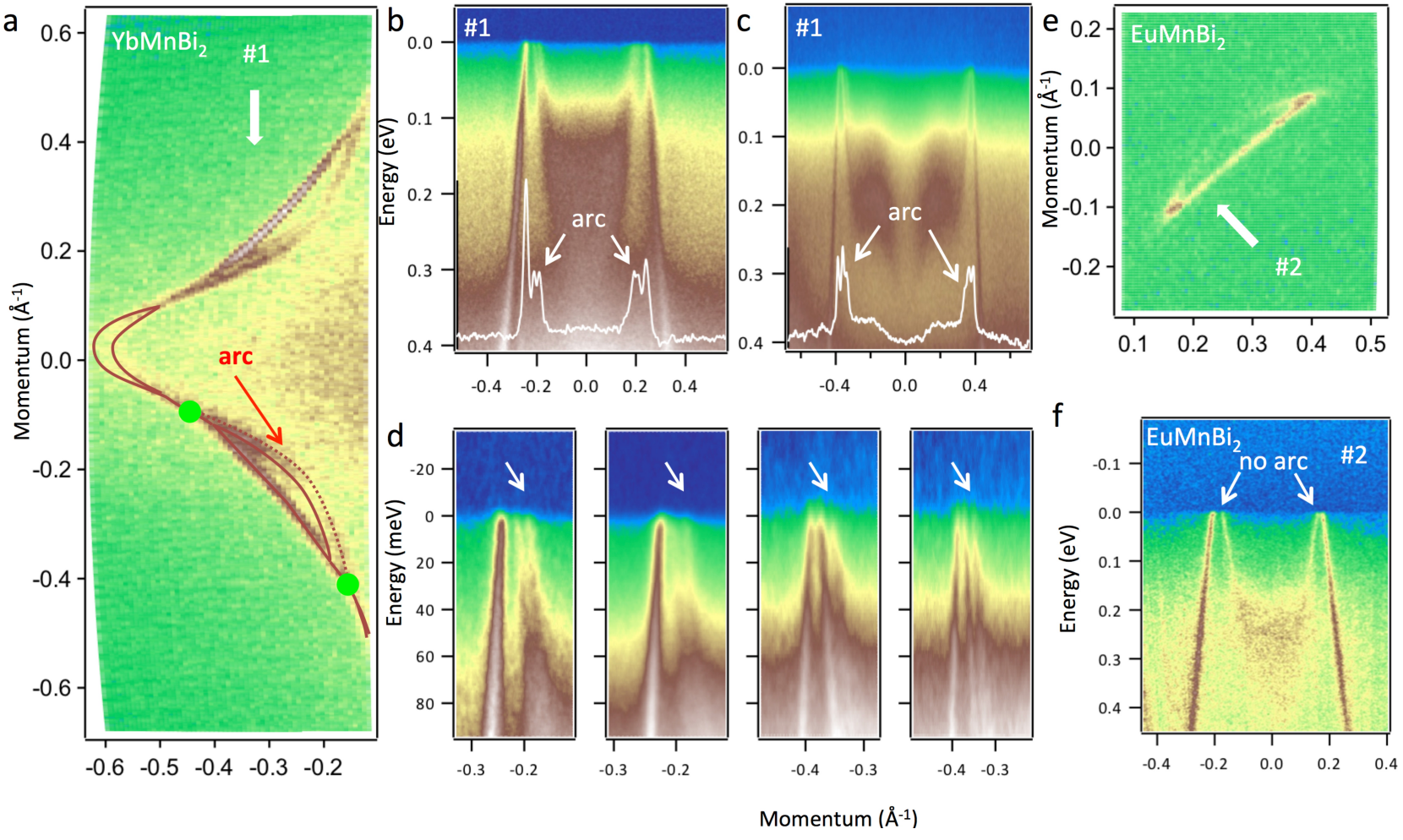

- $YbMnBi_2$: additional 3-rd feature (Fermi arc? Weyl points?) for each lens
- $EuMnBi_2$: only 2 features

arXiv:1507.04847

$YbMnBi_2$: experimental optical conductivity

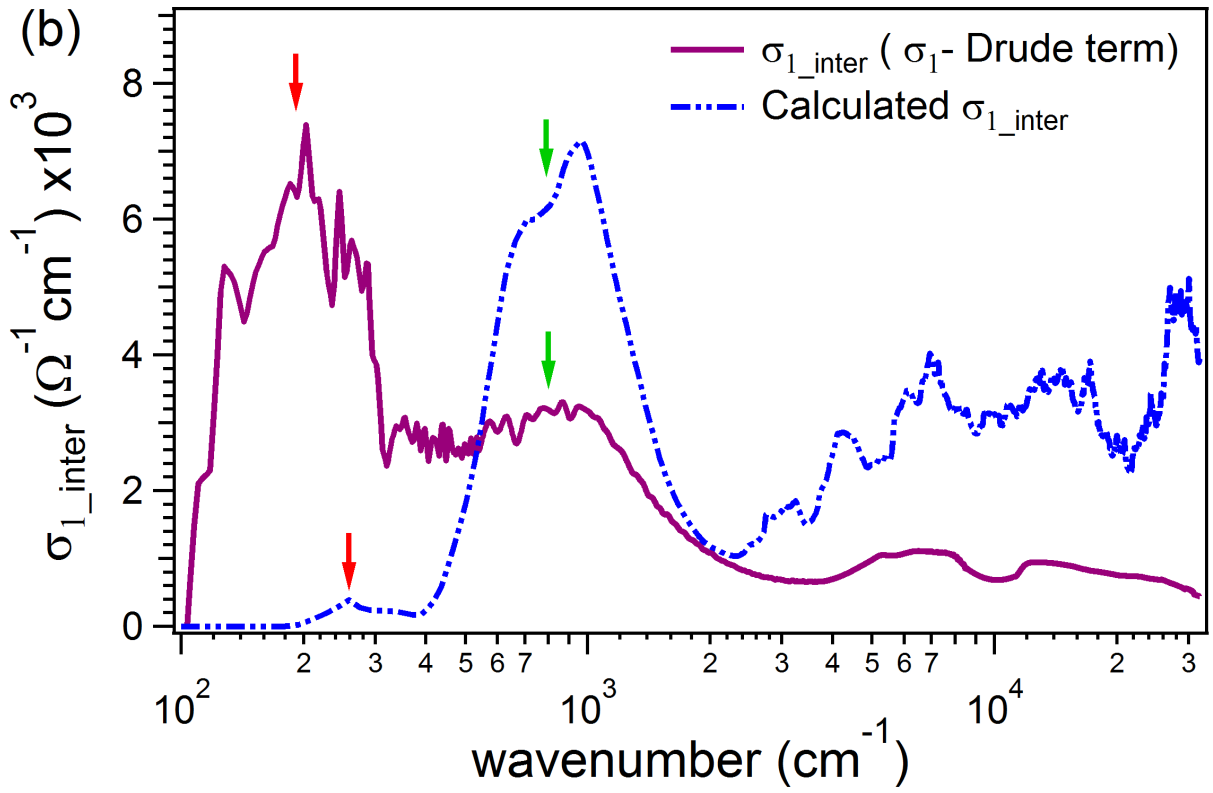

- σ recalculated from reflectivity measurements
- inter-band part after subtraction of intra-band Drude term
- a narrow peak both in the experimental and calculated σ

D. Chaudhuri *et al*, PRB **96**, 075151 (2017)

Where it may come from?

decomposition of σ into inter-band contributions

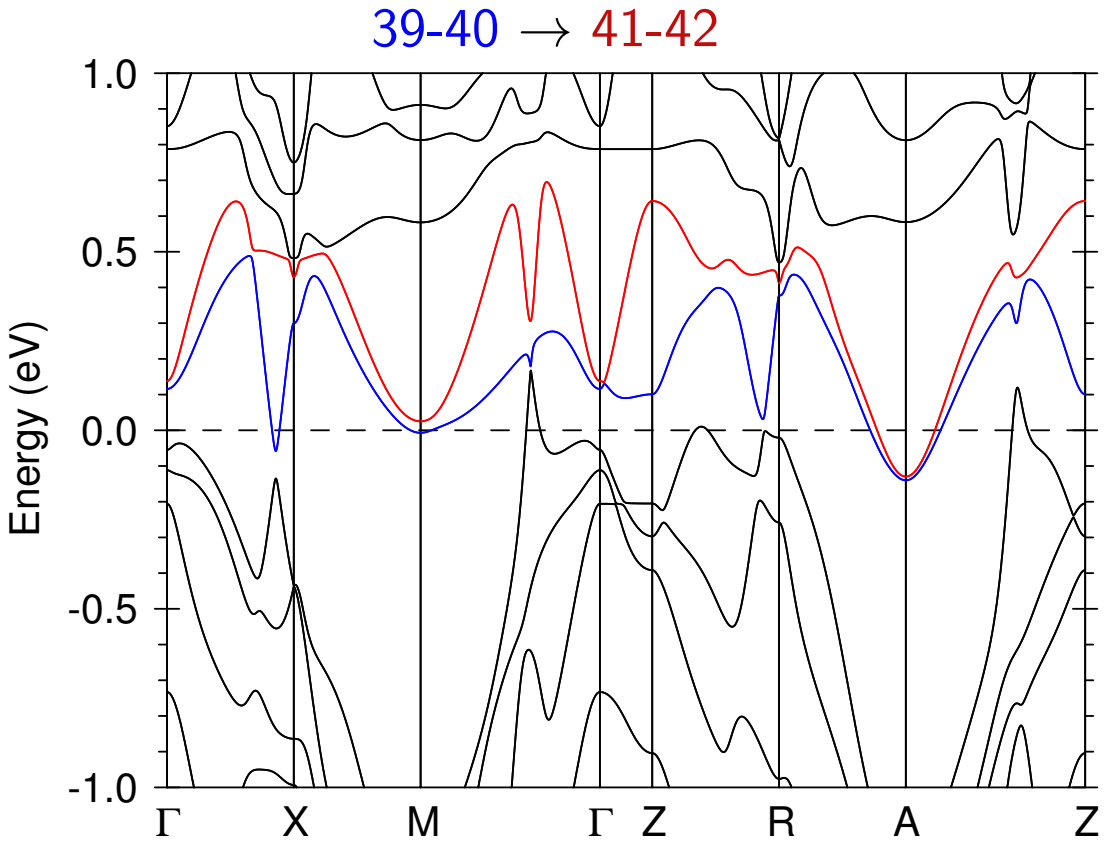

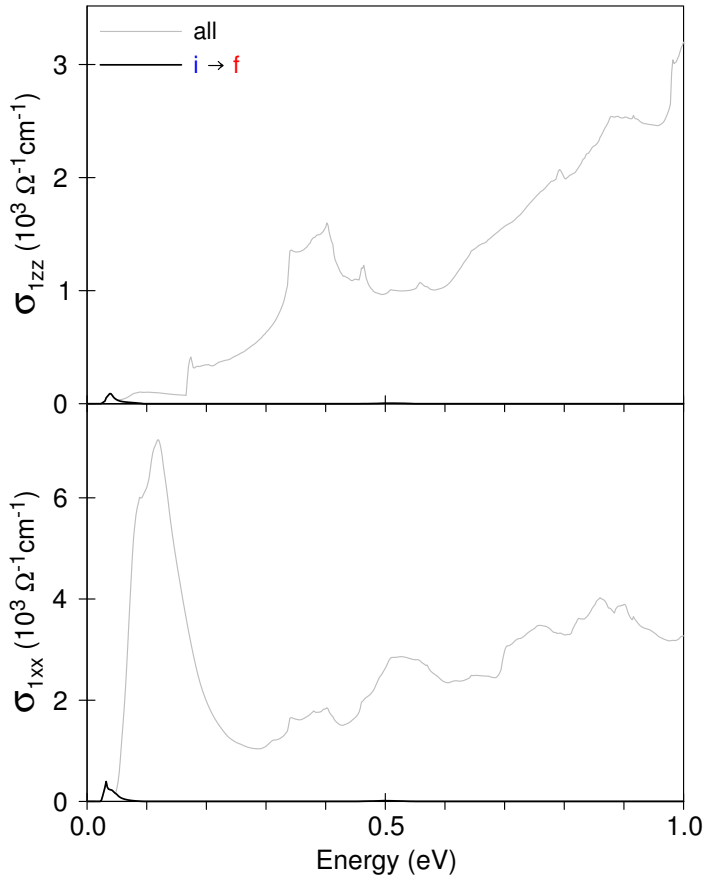

- the peak is due to transitions between Dirac-like bands

decomposition of σ into inter-band contributions

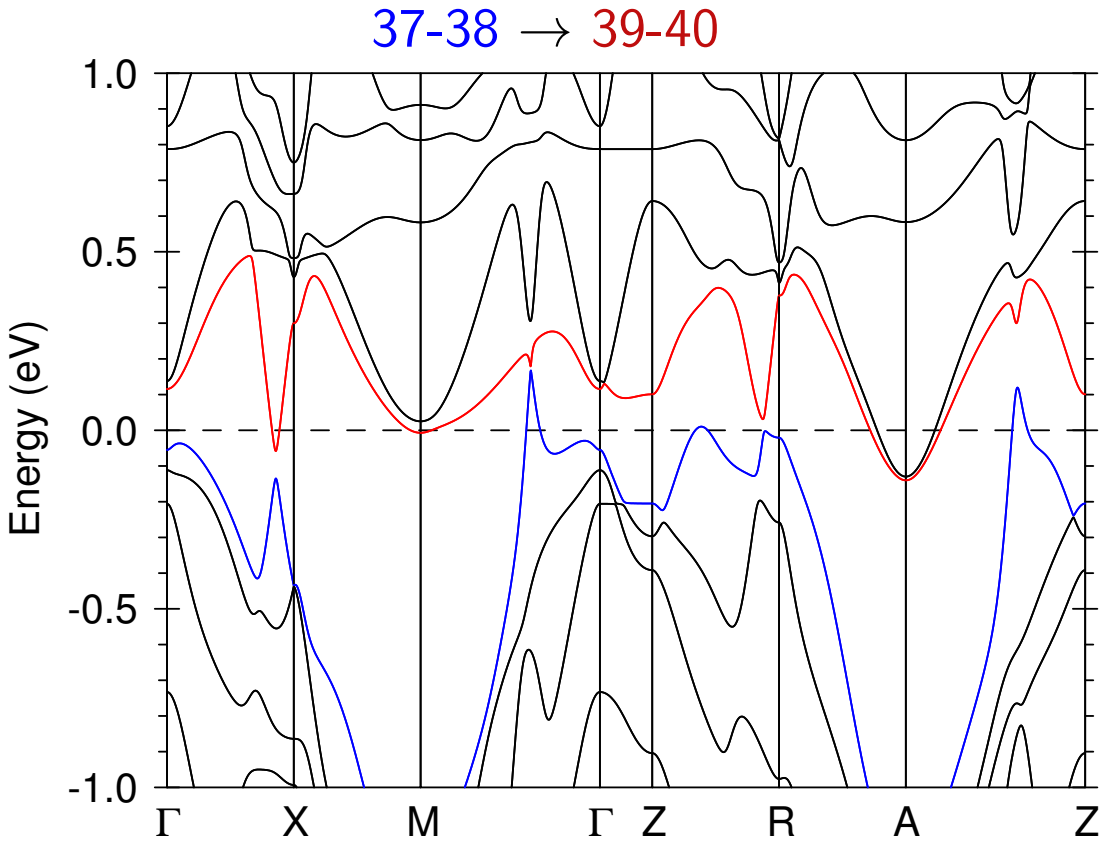

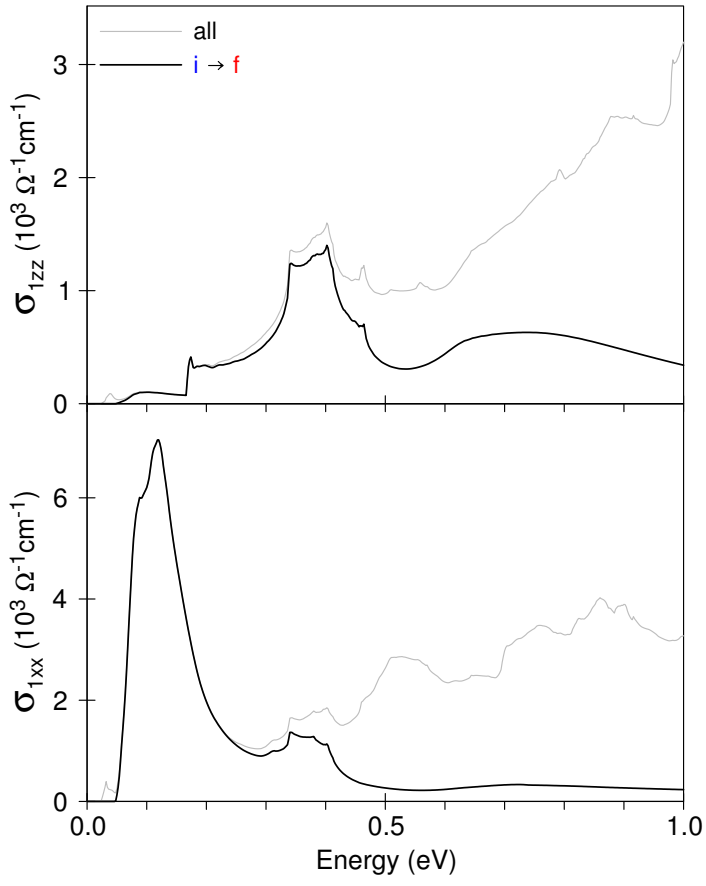

- the peak is due to transitions between Dirac-like bands

decomposition of σ into inter-band contributions

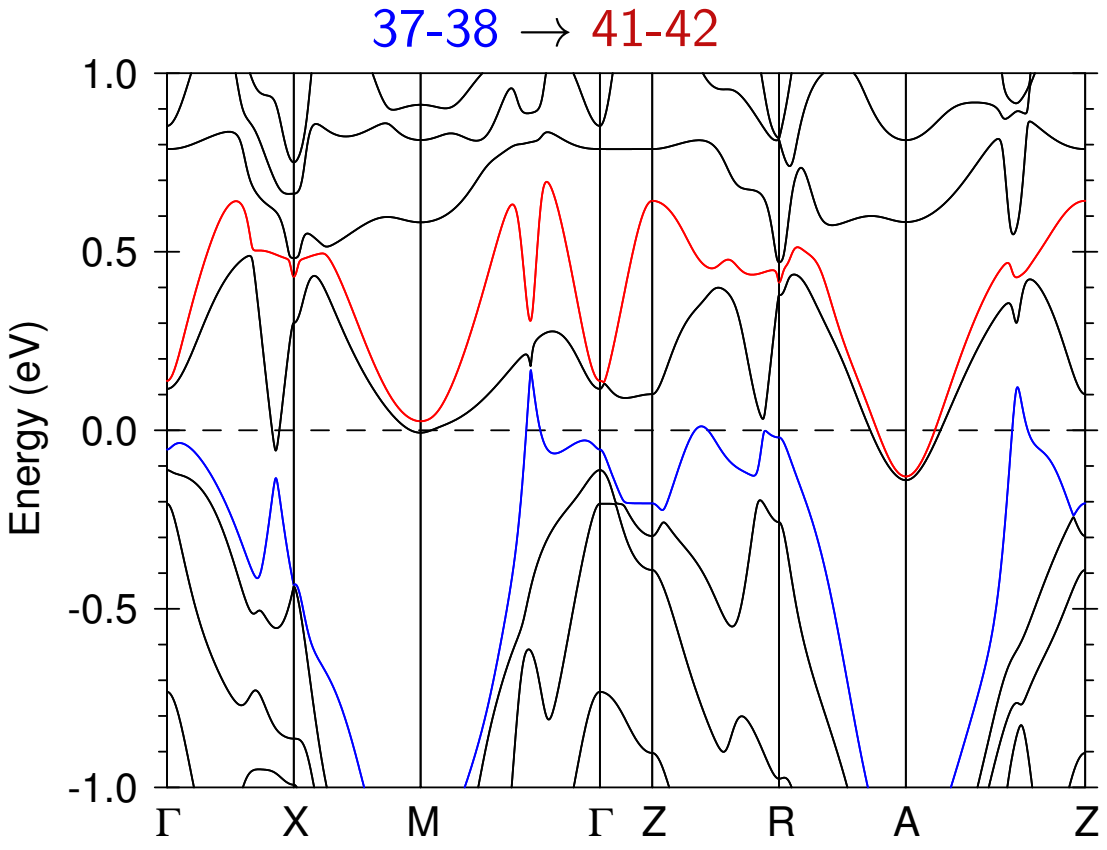

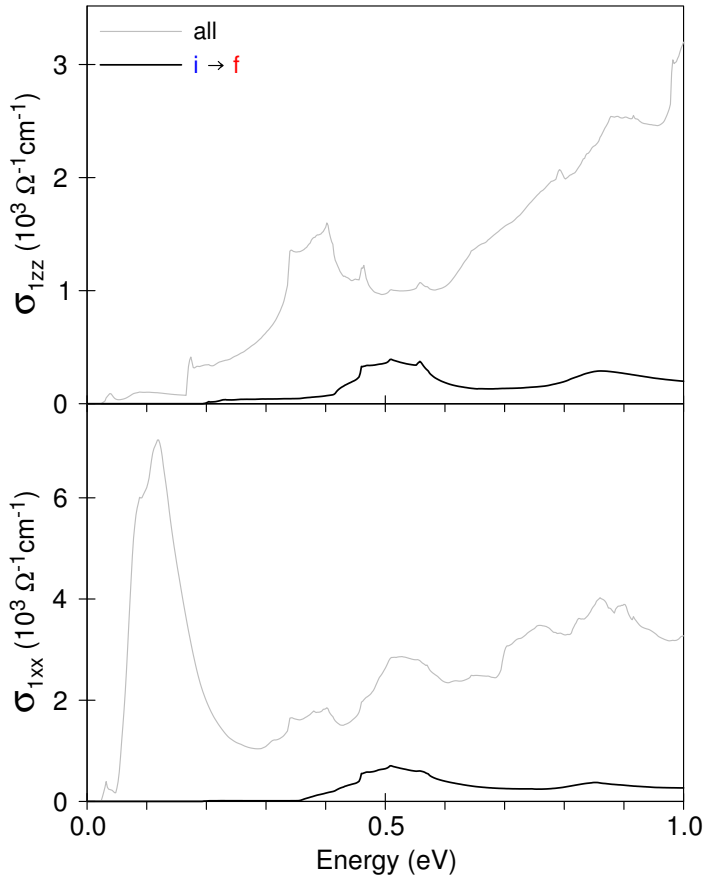

- the peak is due to transitions between Dirac-like bands

contribution from various k-volumes

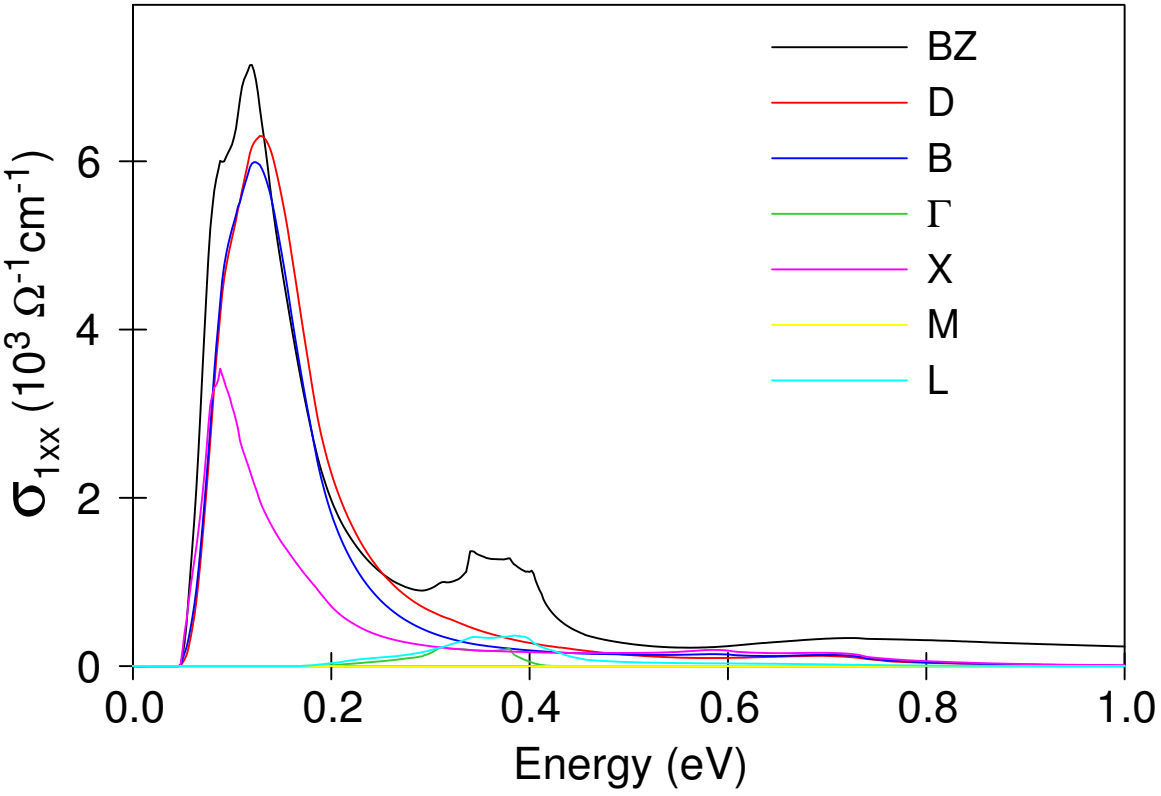

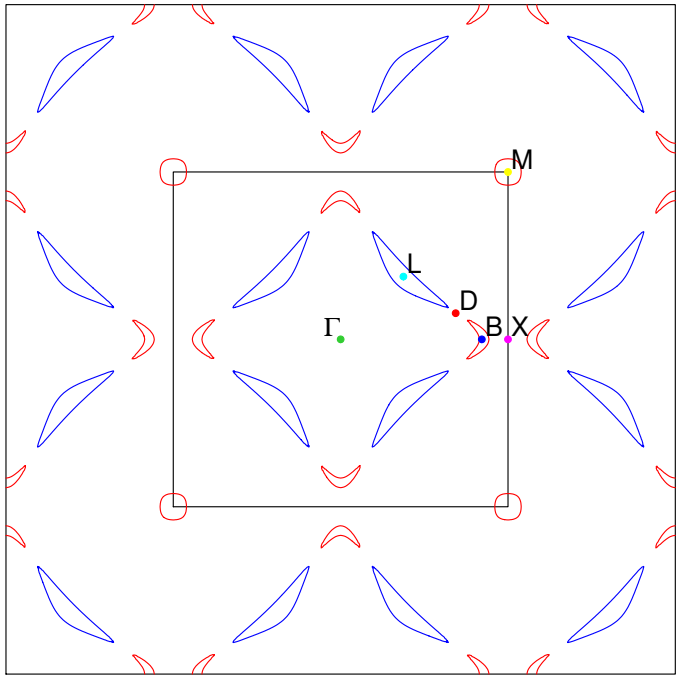

- BZ integration over cylinders in k-space ($r \sim 0.1a^*$)
- dominant contribution from the cylinder centered between "lenses" and "boomerangs"
- transitions between lower and upper of two gapped Dirac bands
- $\hbar\omega_{\text{peak}} \sim \varepsilon_{\text{g}}$ gap between Dirac bands

the gap at $k_z = 0$

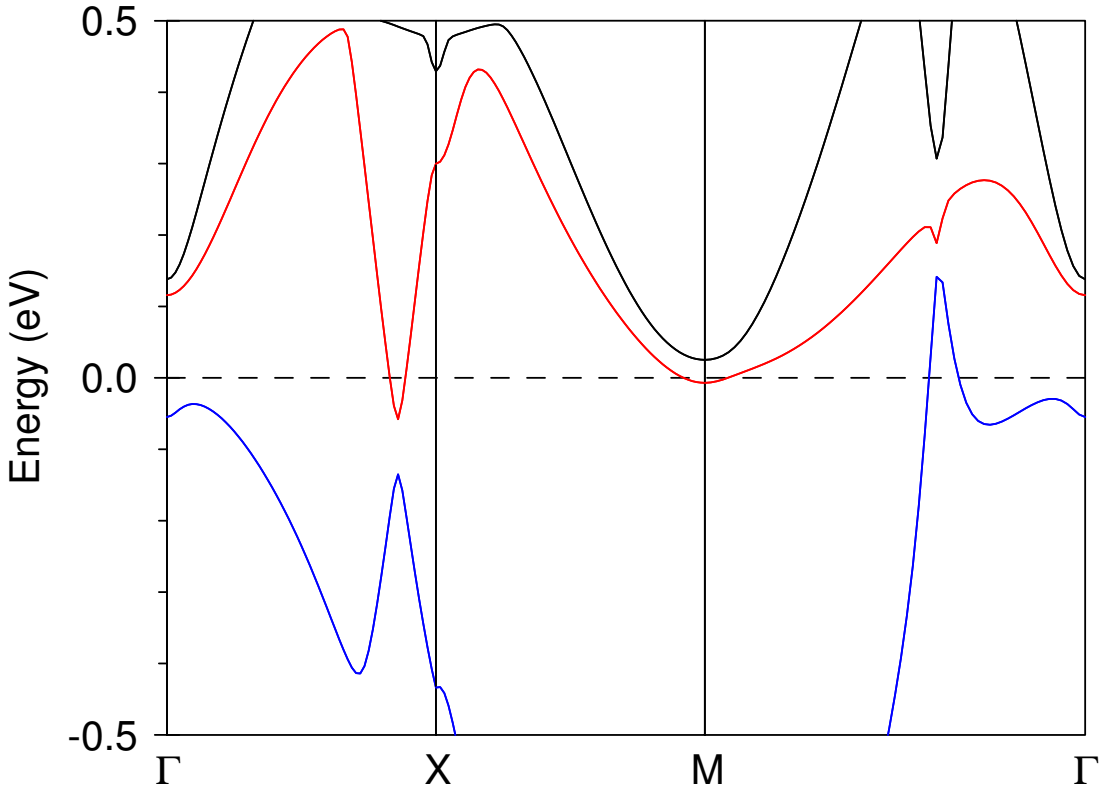

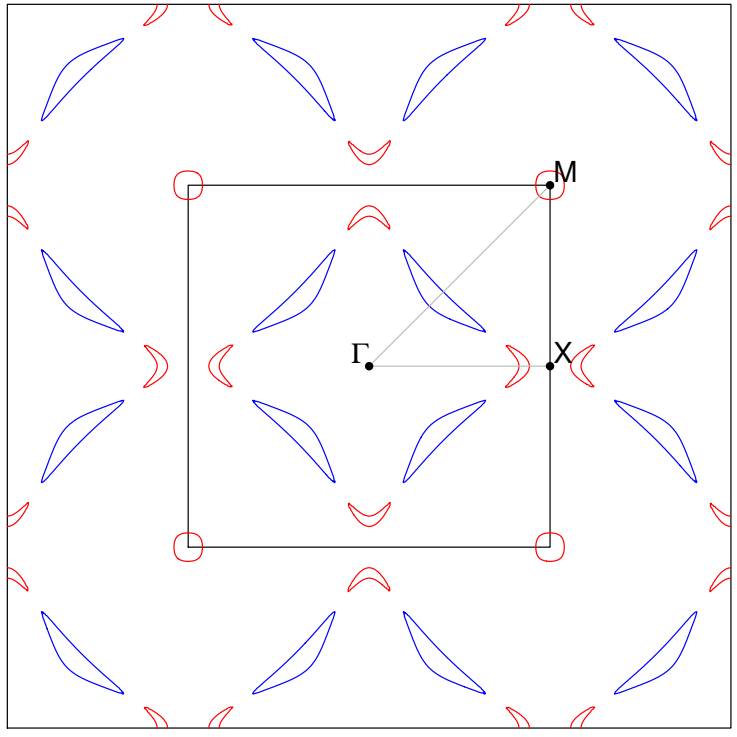

- nearly constant $\varepsilon_g \Rightarrow$ large $\mathbf{k}$ volume for the transitions

the gap at $k_z = 0$

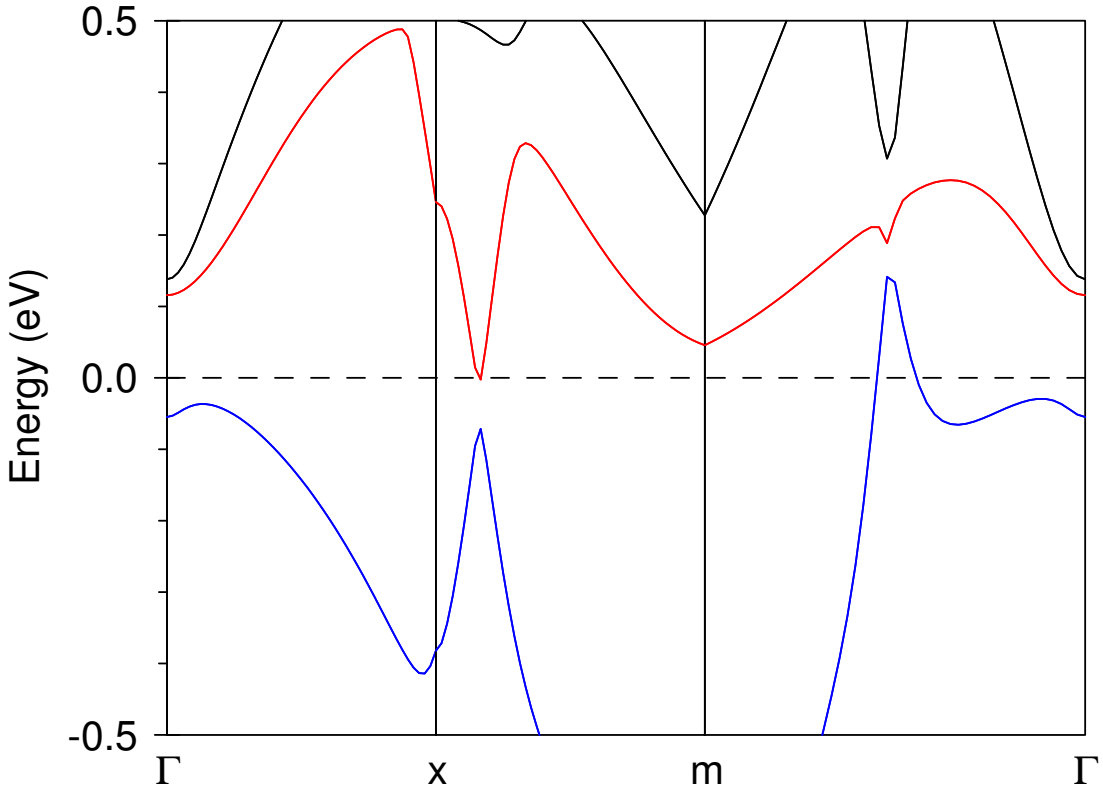

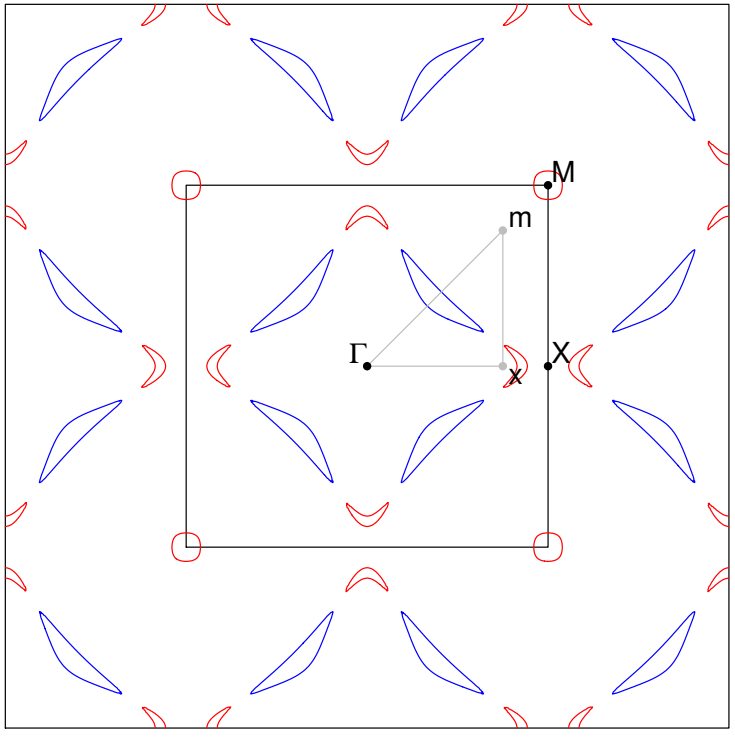

- nearly constant $\varepsilon_g \Rightarrow$ large $\mathbf{k}$ volume for the transitions

extremely slow $\mathbf{k}$ convergence

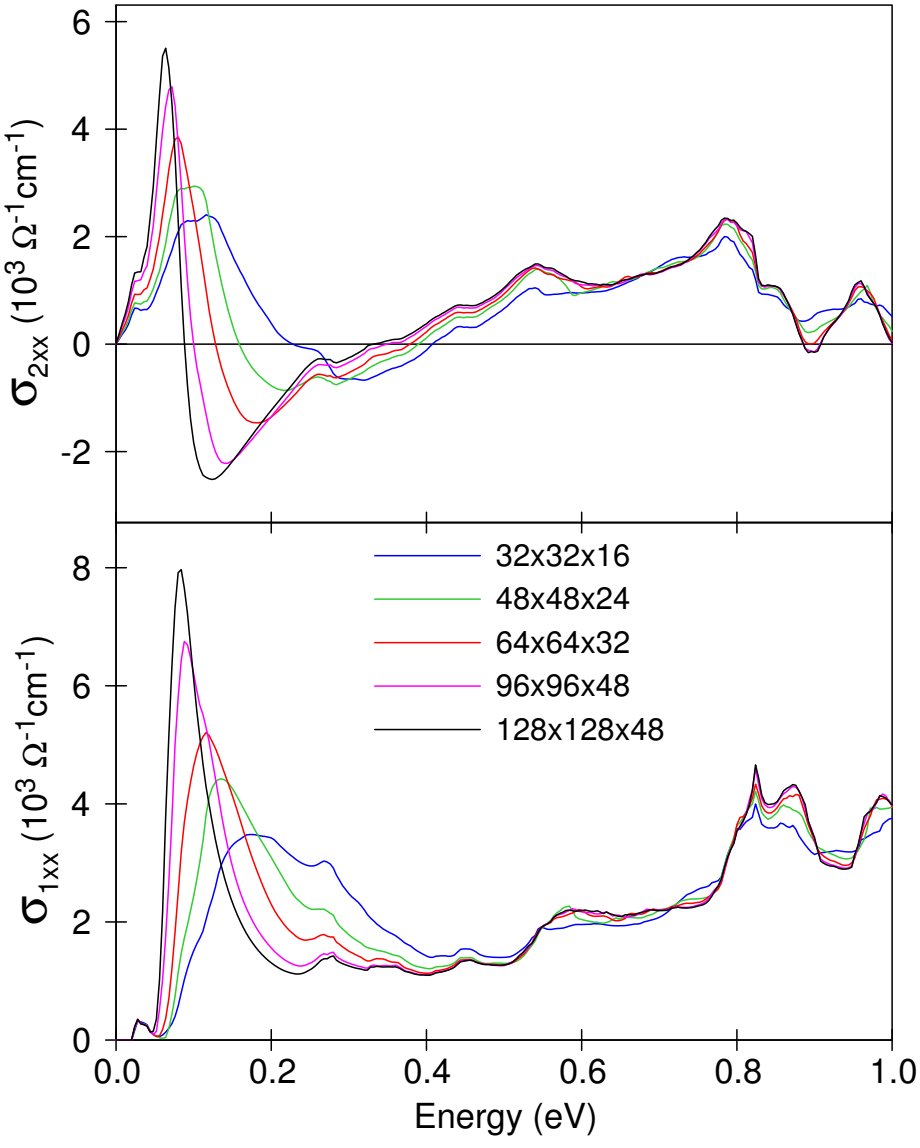

- fine $\mathbf{k}$-mesh in order to resolve the band curvature at the avoided crossing
- usually $32 \times 32 \times 16$ is sufficient
- even for $128 \times 128 \times 48$ mesh convergence is not achieved

1. model optical conductivity
2. a quest for Weyl points in the $YbMnBi_2$
3. low energy peaks in optical conductivity of NbP
4. triple points in GdPtBi

TaAs: Weyl points and Fermi arcs

Fig. 1. Topology and electronic structure of TaAs. (**A**) Body-centered tetragonal structure of TaAs, shown as stacked Ta and As layers. The lattice of TaAs does not have space inversion symmetry. (**B**) STM topographic image of TaAs's (001) surface taken at the bias voltage −300 mV, revealing the surface lattice constant. (**C**) First-principles band structure calculations of TaAs without spin-orbit coupling. The blue box highlights the locations where bulk bands touch in the BZ. (**D**) Illustration of the simplest Weyl semimetal state that has two single Weyl nodes with the opposite (±1) chiral charges in the bulk. (**E**) In the absence of spin-orbit coupling, there are two line nodes on the k_x mirror plane and two line nodes on the k_y mirror plane (red loops). In the presence of spin-orbit coupling, each line node reduces into six Weyl nodes (small black and white circles). Black and white show the opposite chiral charges of the Weyl nodes. (**F**) A schematic (not to scale) showing the projected Weyl nodes and their projected chiral charges. (**G**) Theoretically calculated band structure (*26*) of the Fermi surface on the (001) surface of TaAs. (**H**) The ARPES-measured Fermi surface of the (001) cleaving plane of TaAs. The high-symmetry points of the surface BZ are noted.

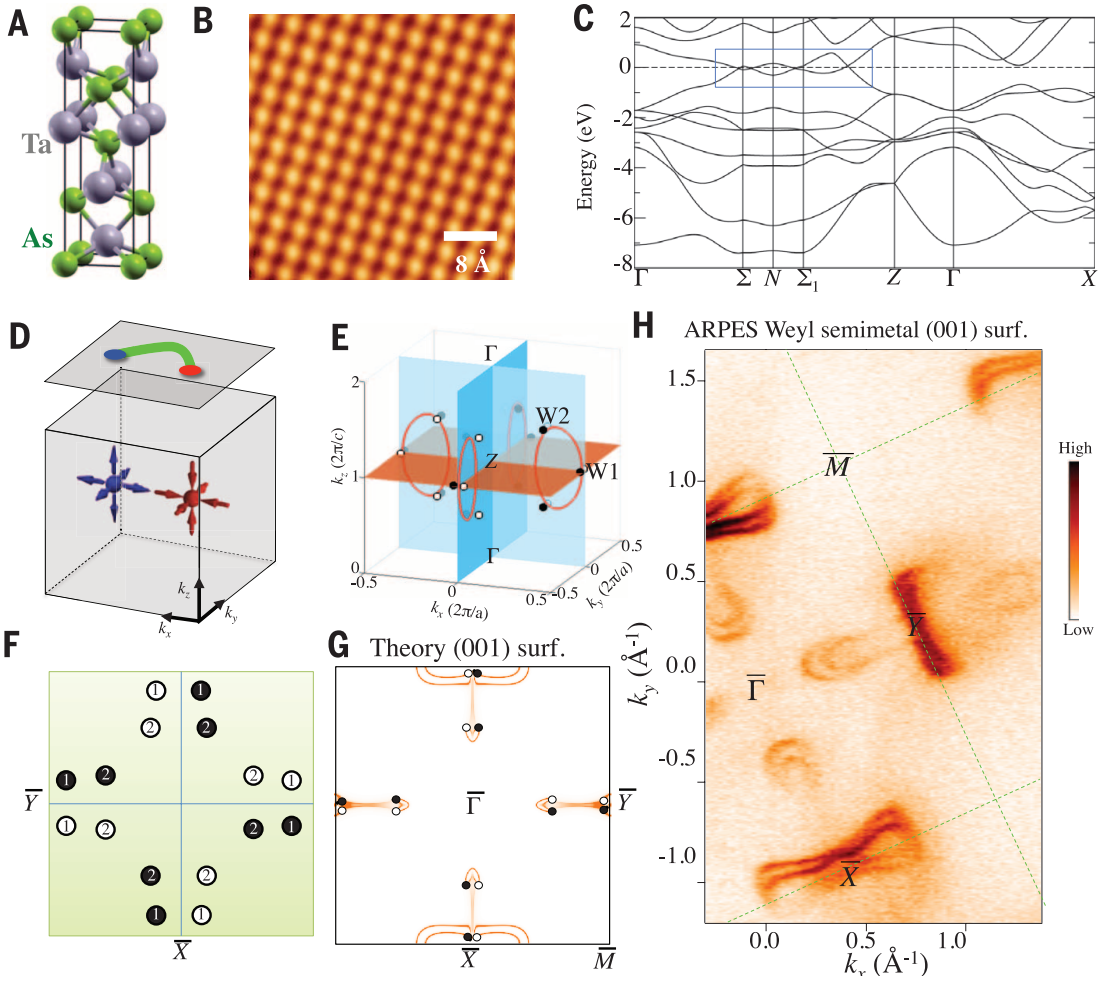

S.-Y. Xu *et al*, Science **349**, 613 (2015)

NbP: line nodes and Weyl points

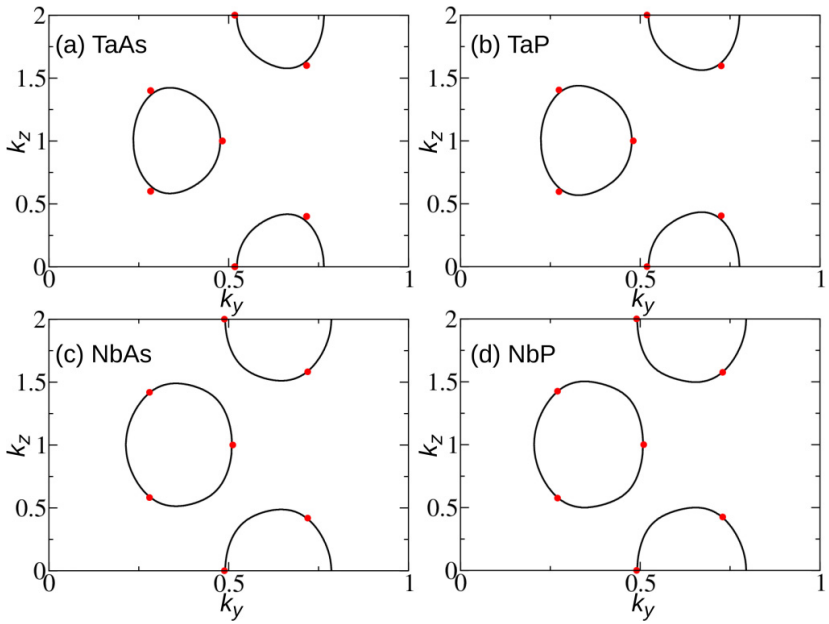

FIG. 6. (Color online) Line nodes on the $k_x = 0$ plane formed by the crossing of valence and conduction bands in (a) TaAs, (b) TaP, (c) NbAs, and (d) NbP without spin-orbit coupling. The red solid circles indicated the projection of Weyl nodes on the $k_x = 0$ plane after turning on the spin-orbit coupling. For each circle, two Weyl nodes of opposite chiralities on two sides of the $k_x = 0$ plane are found.

TABLE II. The coordinates (in units of reciprocal lattice vectors of the conventional unit cell) and energies (in eV) of two representative distinct Weyl nodes denoted W_1 and W_2. In each compound the energy of W_2 is higher than that of W_1. Here, $\pm$ stands for a mirror pair of Weyl nodes.

	Coordinate of W_1	Energy of W_1
TaAs	$(\pm 0.0072, 0.4827, 1.0000)$	-0.0221
TaP	$(\pm 0.0074, 0.4809, 1.0000)$	-0.0531
NbAs	$(\pm 0.0025, 0.5116, 1.0000)$	-0.0322
NbP	$(\pm 0.0028, 0.5099, 1.0000)$	-0.0534
	Coordinate of W_2	Energy of W_2
TaAs	$(\pm 0.0185, 0.2831, 0.6000)$	-0.0089
TaP	$(\pm 0.0156, 0.2743, 0.5958)$	0.0196
NbAs	$(\pm 0.0062, 0.2800, 0.5816)$	0.0042
NbP	$(\pm 0.0049, 0.2703, 0.5750)$	0.0259

Chi-Cheng Lee, *et al*, PRB **92**, 235104 (2015)

NbP: scalar-relativistic fat bands and FS

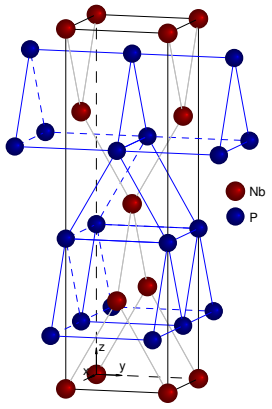

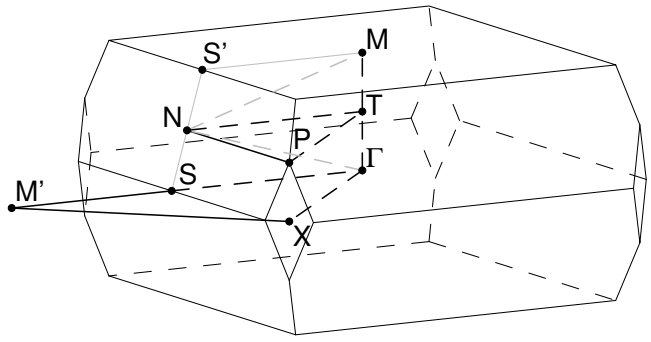

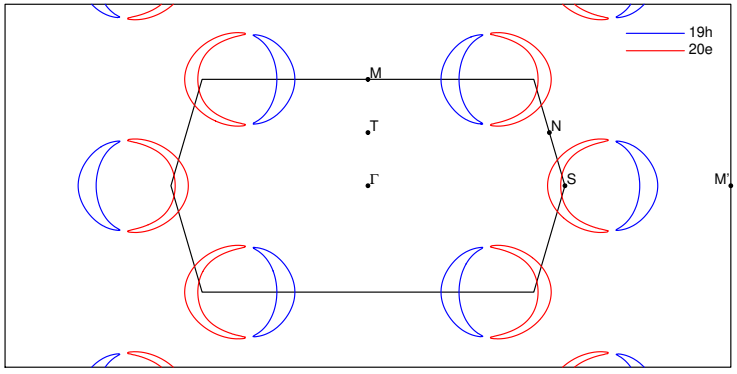

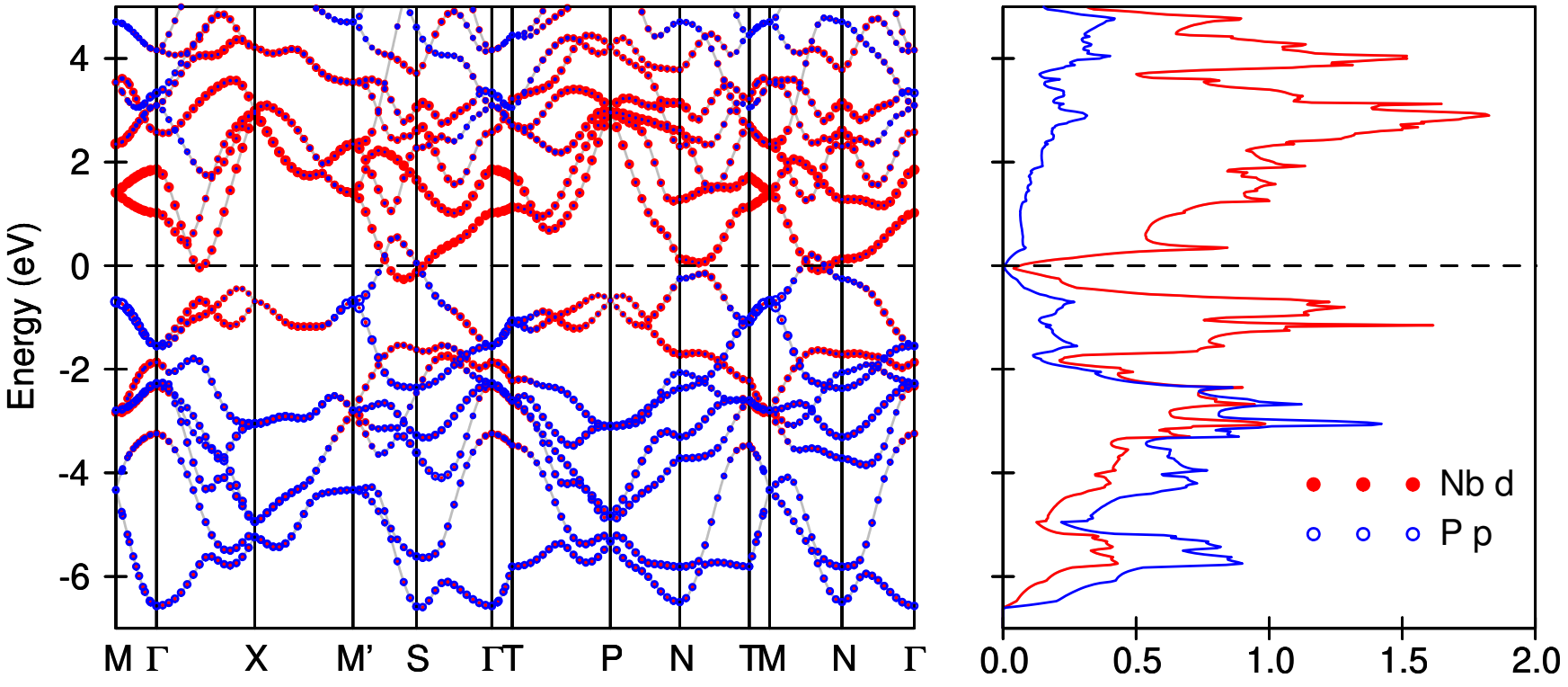

NbP: optical conductivity

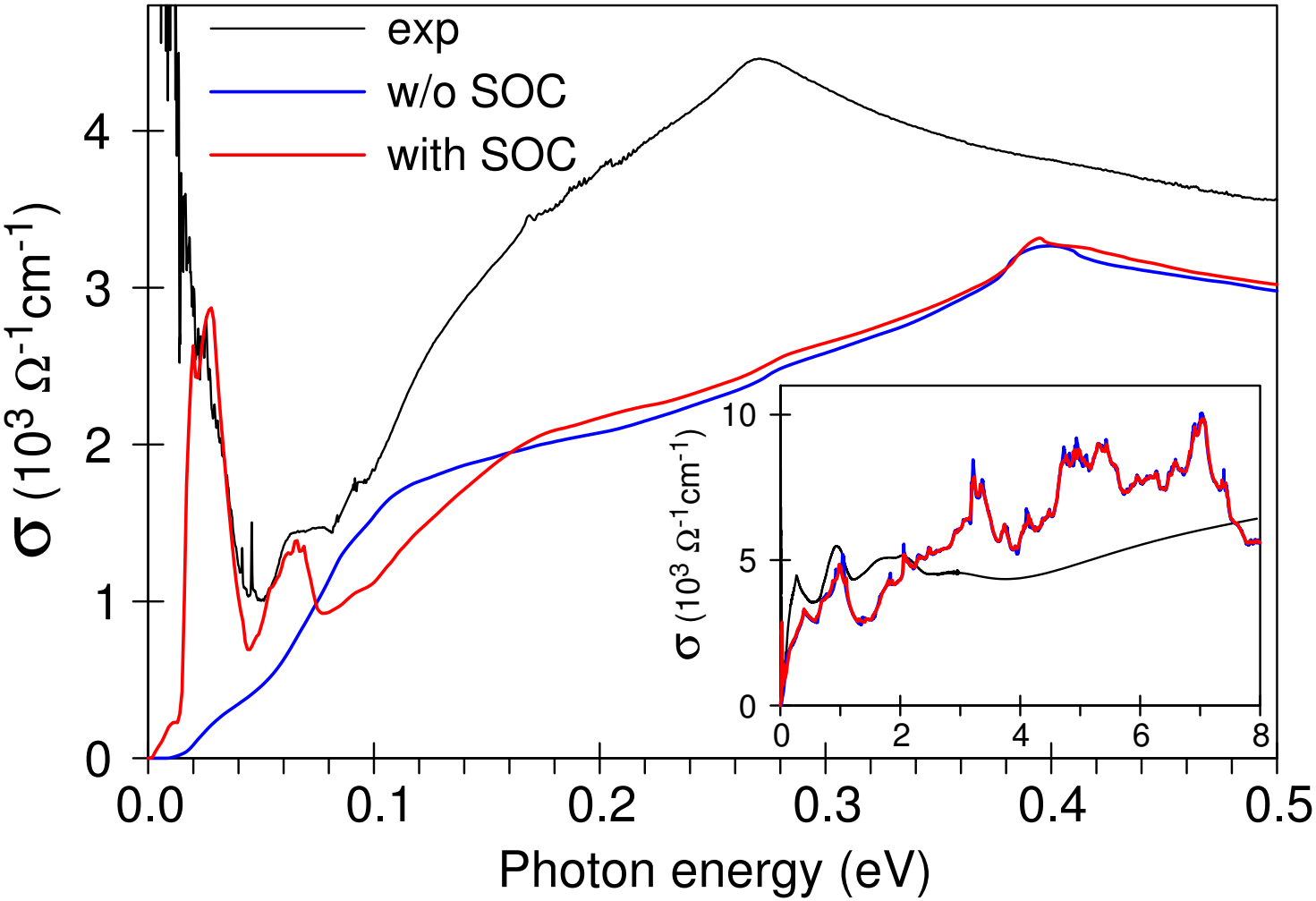

- nearly linear $\sigma(\omega)$ below 0.15 eV
- masked by two intense peaks at 0.03 and 0.06 eV

D. Neubauer, *et al*, PRB **98**, 195203 (2018)

NbP: bands and Fermi surface with SOC

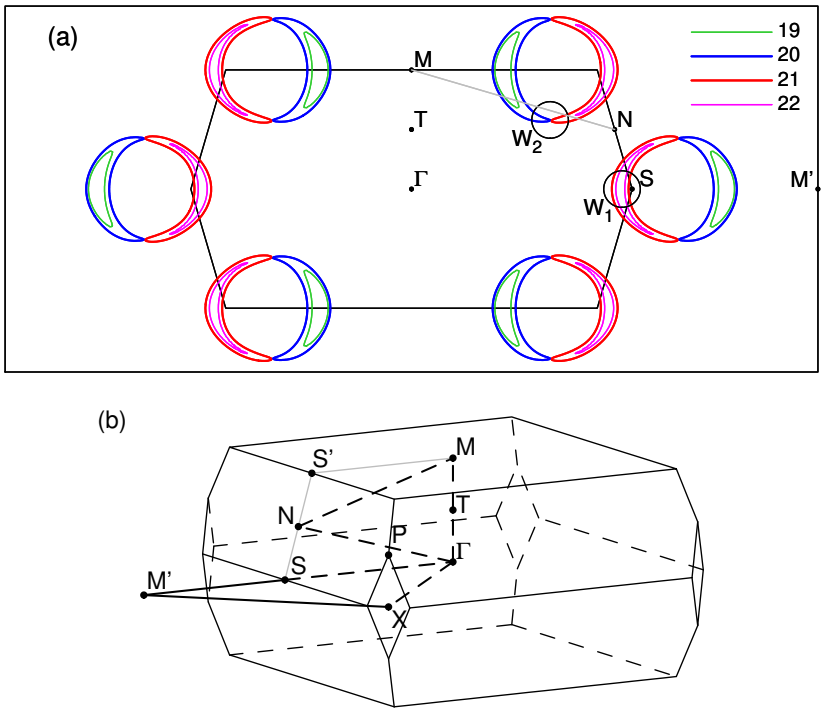

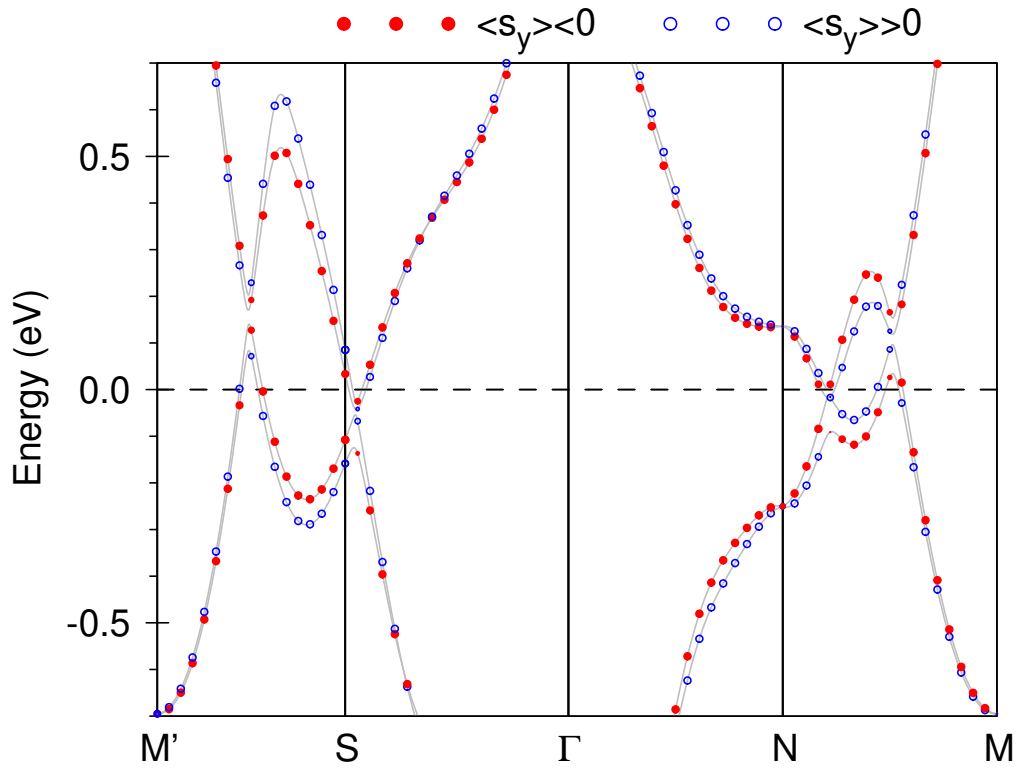

- SOC lifts 2-fold band degeneracy
- SOC split bands with nearly parallel dispersion cross E_F
- $|\langle s_y \rangle| \sim \frac{1}{2}$ away from crossing points
- weak dipole transitions between bands with opposite spins

NbP: origin of the low energy peaks

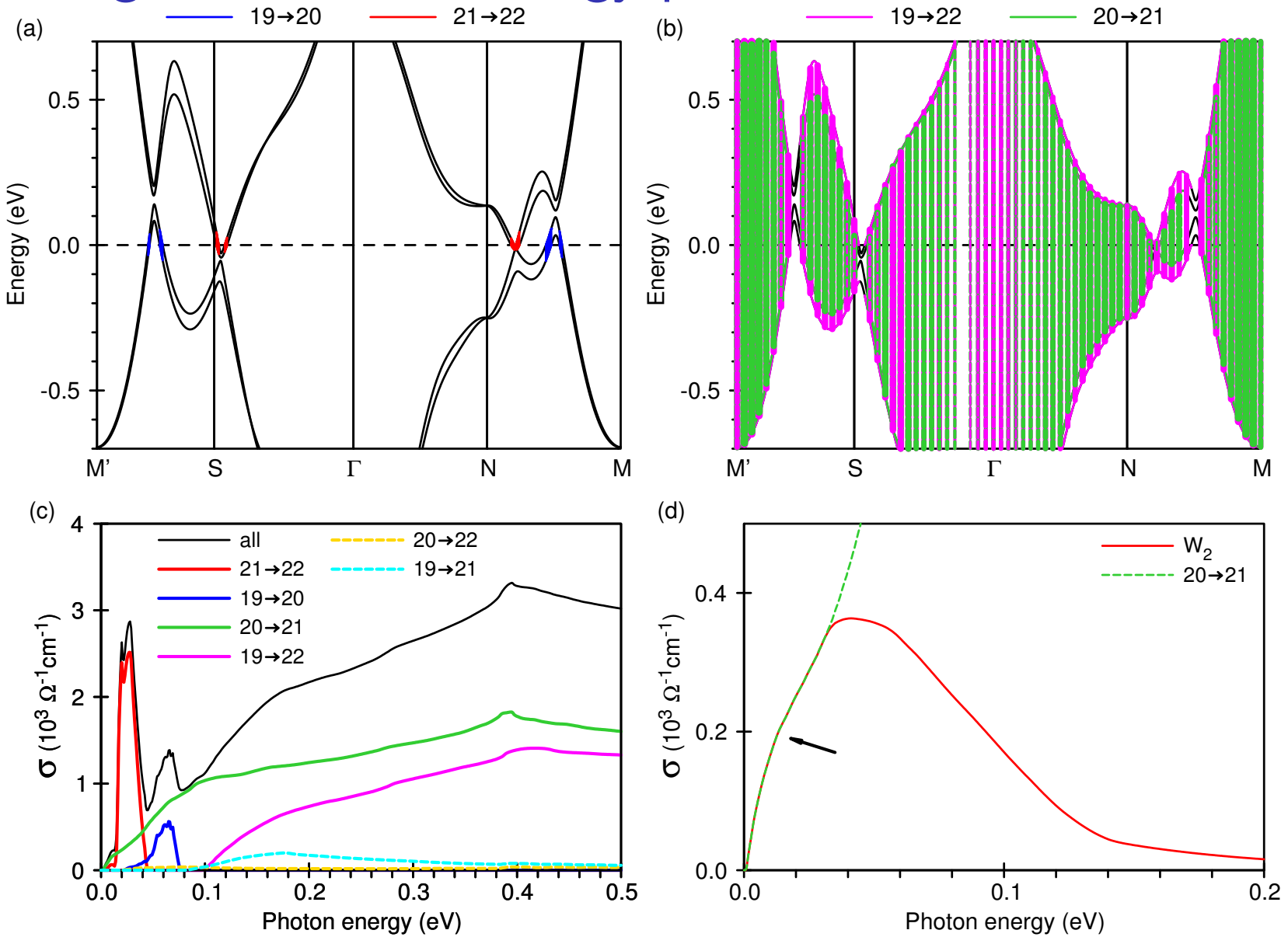

- $19 \rightarrow 20$ and $21 \rightarrow 22$ transitions between nearly parallel SOC split bands

D. Neubauer, *et al*, PRB **98**, 195203 (2018)

1. model optical conductivity
2. a quest for Weyl points in the $YbMnBi_2$
3. low energy peaks in optical conductivity of NbP
4. triple points in GdPtBi

GdPtBi

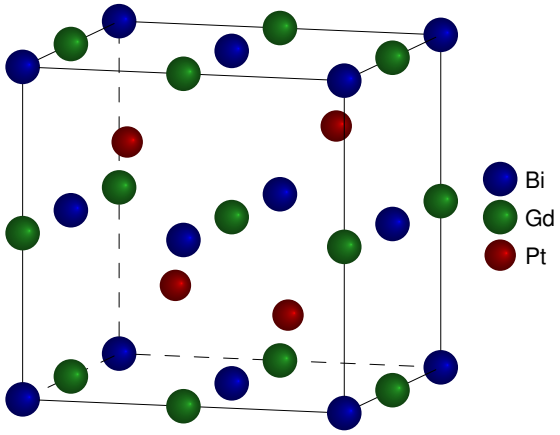

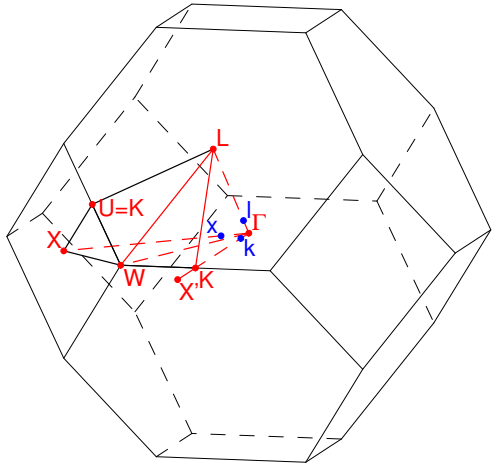

- cubic half-Heusler structure
- 4-fold degeneracy at Γ
- triple point along Γ–L
- semi-core Gd $4f$;
  spin-polarization is neglected

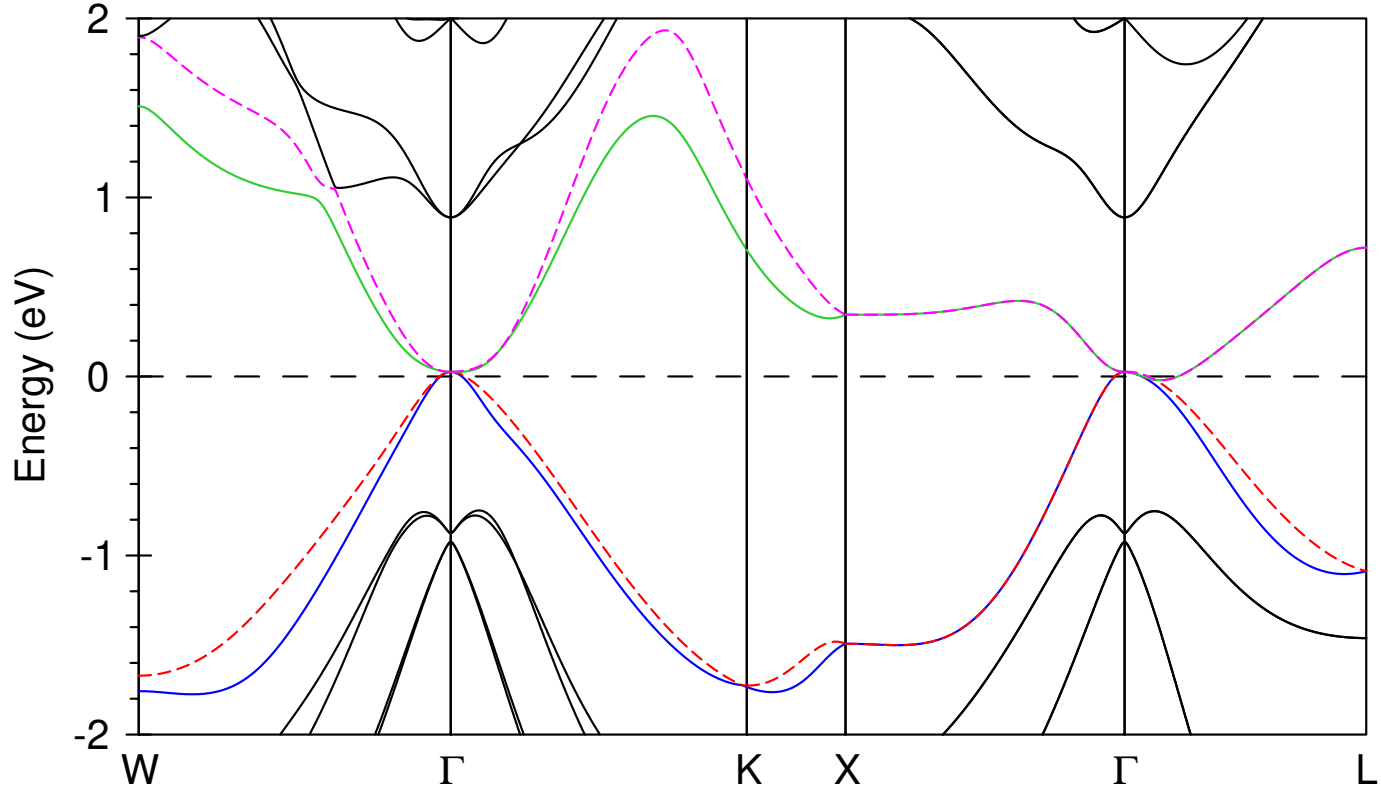

GdPtBi: optical conductivity

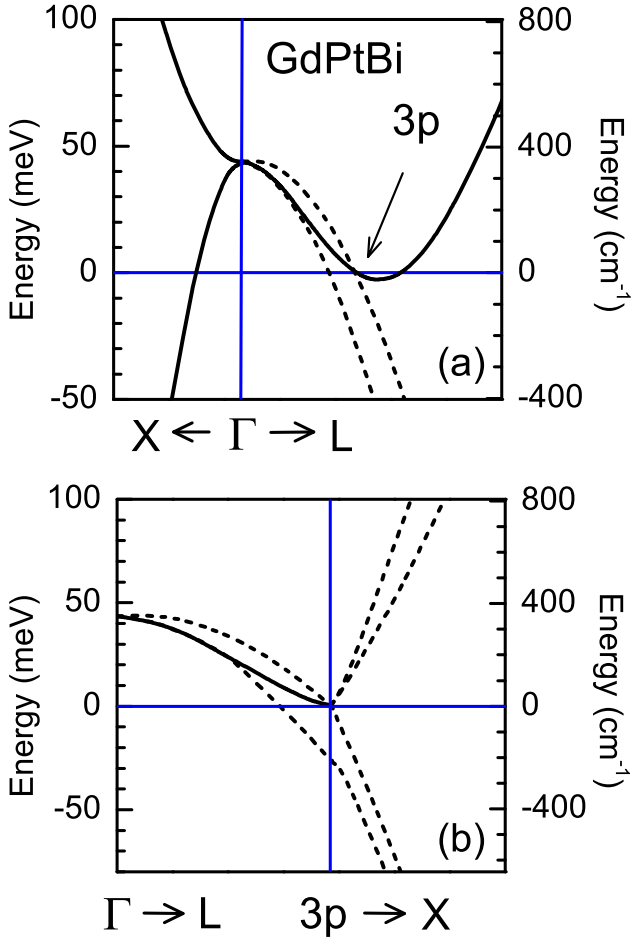

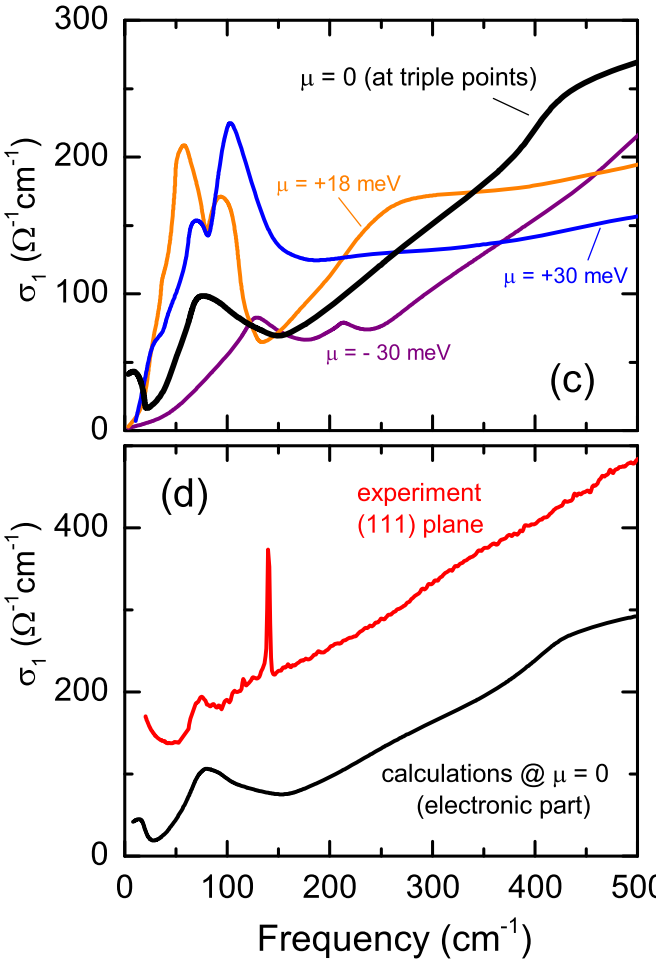

- exp: linear $\sigma(\omega)$ in a wide ω range (above $T_C \sim 10$ K)
- calc: strong dependence on the Fermi level (μ) position
- calc: linear $\sigma(\omega)$ due to nearly linear band dispersion $\perp$ Γ–L

F. Hütt, *et al*, PRL **121**, 176601 (2018)

conclusions

- $YbMnBi_2$: the narrow peak of the optical conductivity appears due to inter-band transitions across the gapped "line nodes"; even if it is there, linear $\sigma(\omega)$ is masked by the peak
- NbP: intense inter-band peaks between nearly parallel SOC-spit bands mask linear $\sigma(\omega)$
- GdPtBi: triple points but linear $\sigma(\omega)$

collaborators

ARPES, theory:

S. Borisenko, D. Evtushinsky, K. Koepernik, J. van den Brink, B. Büchner
IFW, Dresden,Germany

T. Kim, M. Hoesch
Diamond Light Source, Didcot, United Kingdom

optics:

D. Chaudhuri, B. Cheng, N. P. Armitage
Department of Physics and Astronomy, The Johns Hopkins University, Baltimore, USA

D. Neubauer, W. Li, A. Löhle, R. Hübner, F. Hütt, M.B. Schilling, A. Pronin, M. Dressel
1. Physikalisches Institut, University of Stuttgart, Germany

samples:

M. Ali, Q. Gibson, R. J. Cava
Department of Chemistry, Princeton University, USA

C. Shekhar, C. Felser
Max Planck Institut for Chemical Physics of Solids, Dresden, Germany